UCRL-ID-119548

Marshak Waves: Constant Flux vs. Constant T - a (slight) Paradigm Shift

Mordecai D. Rosen

December 22, 1994

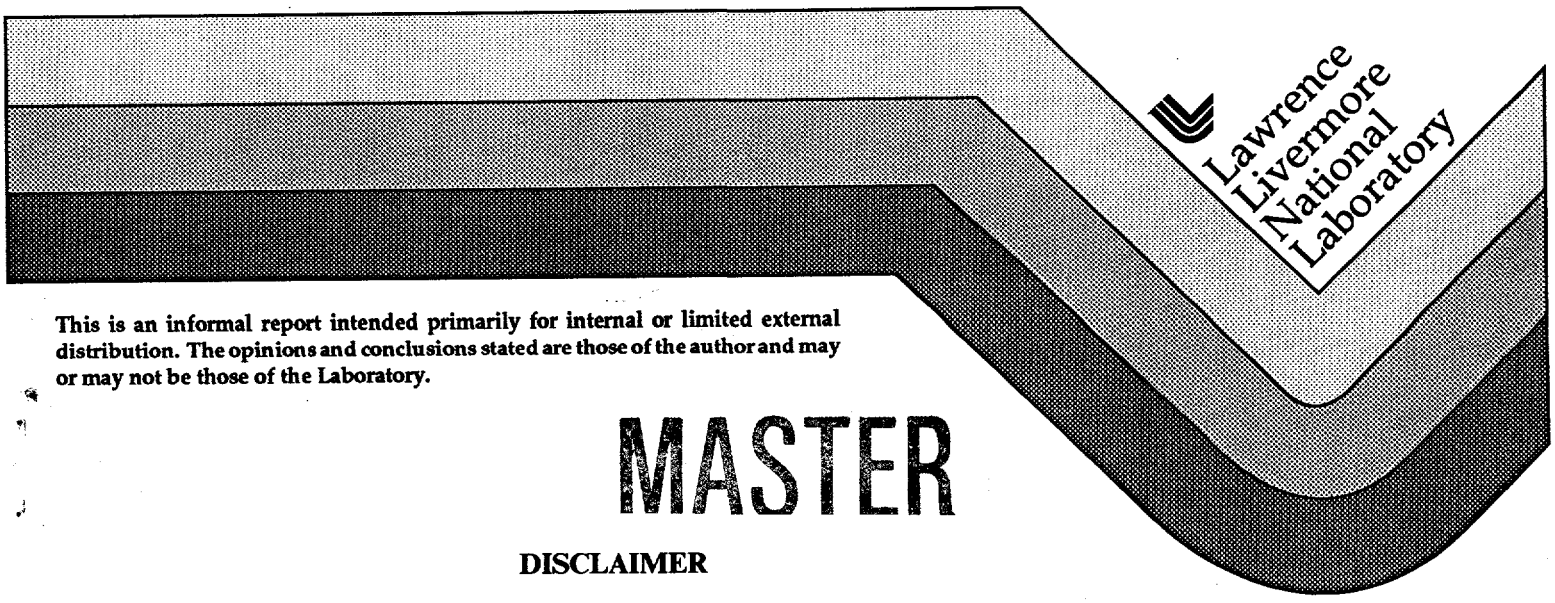

DISCLAIMER

Marshak Waves: Constant Flux vs. Constant T - a (slight) Paradigm Shift

Mordecai D. Rosen
ICF Target Physics Program
Lawrence Livermore National Laboratory
Livermore, CA 94550

ABSTRACT

We review the basic scaling laws for Marshak waves and point out the differences in results for wall loss, albedo, and Marshak depth when a constant absorbed flux is considered as opposed to a constant absorbed temperature. Comparisons with LASNEX simulations and with data are presented that imply that a constant absorbed flux is a more appropriate boundary condition.(U)

I. Introduction

Understanding the radiation drive in laser heated hohlraums is a crucial first step in building confidence in the predicted target performance for a National Ignition Facility (NIF) ignition target. In this paper we will review the basic theory of hohlraum drive scaling, and compare results for the wall loss due to radiation diffusion derived by assuming a constant temperature boundary condition compared to a constant absorbed flux boundary condition. We will also present temperature data and simulations from hohlraums driven by 1 nsec flat top laser drives which will imply that the constant absorbed flux boundary condition is the more appropriate one. In addition we will present simulations and measurements of the radiation burn- through times through thin patches of Au on the sides of a hohlraum wall, which also lead to the same conclusion.

In ICF hohlraums (mm scale gold cylinders), laser light enters the hohlraum interior through laser entrance holes located in either end cap of the cylinder. The light is absorbed at the cylinder walls, converting laser light into soft x-rays. These x-rays are rapidly absorbed and reemitted by the walls setting up a radiation driven thermal wave[1] diffusing into the

walls (a so called "Marshak Wave"). Some of the x-rays escape out the laser entrance holes while others are absorbed by the target capsule and drive its implosion. In Section II the basic scaling of hohlraum wall loss due to the Marshak Wave will be derived. As an aside, basic and useful concepts such as wall reflectivity (albedo) will be presented. In Section III methods of measuring hohlraum drive will be described. Results from 1 nsec flat top laser drives will also be presented there. Sophisticated LASNEX simulations will be presented there as well, which show excellent detailed agreement with the drive measurements. Radiation burn-through experiments dedicated to separately measuring wall loss will be described in Section IV as well as LASNEX simulations that agree very well with the burn-through data. In Section V we will summarize our findings that on the basis of the data and simulations of Sections III and IV, the constant absorbed flux boundary condition is the appropriate one to use.

II. Marshak Wave Scaling

The theory will be presented here in steps, building up complexity so that the reader can keep up with the understanding of the issues and results. The model system under consideration is a heat wave driven by a radiant flux impinging on a material boundary at x=0 and at t=0, and penetrating into that material. Since the x-rays are constantly being reabsorbed and reemitted as they progress deeper into the material, a classical diffusive situation arises. We seek to find an expression for the temperature profile T(x,t) within that material at any deeper position x and subsequent time t. To do so we must solve a basic diffusion equation, which is always in the form:

$$\frac{\partial}{\partial t}\begin{pmatrix} energy \\ density \end{pmatrix} = \frac{\partial}{\partial x}\begin{pmatrix} energy \\ flux \end{pmatrix} = \frac{\partial}{\partial x}\left[D \frac{\partial}{\partial x}\begin{pmatrix} energy \\ density \end{pmatrix}\right] \qquad (1)$$

where here the energy density on the lhs of the equation is the matter energy density, $\rho\varepsilon$, where ρ is the matter density and ε is the specific matter energy. The energy flux, however, is carried by thermal radiation, hence the energy density on the rhs of the equation is radiant energy density aT^4, and the diffusion coefficient D is given, as always, by a free streaming velocity, (in this case, c, the speed of light) times 1/3 of a mean free path, which for optically thick systems is the Rosseland mean free path λ_R. Thus Eq. (1) becomes:

$$\frac{\partial}{\partial t}(\rho\varepsilon)=\frac{\partial}{\partial x}\left[\frac{c\lambda_R}{3}\frac{\partial}{\partial x}(aT^4)\right]\propto\frac{\partial}{\partial x}\left[\frac{\sigma T^4}{x/\lambda_R}\right] \qquad (2)$$

where the Stephan Boltzman constant $\sigma = ac/4$. The second half of Eq. (2) serves as a reminder to the reader that in radiation diffusion, as in any diffusion, diffusive flux is free streaming flux reduced by the number of mean free paths in the system. Further progress can be made by fitting powers of T into power laws for the key variables, ε and λ_R. To simplify the problem for the moment, we will assume the density of the matter stays constant in time and space: $\rho=\rho_0$, and that the temperature at the material boundary T_0 is constant in time: $T(x=0,t)= T_0t^0$. Thus we set $\varepsilon = \varepsilon_0T^l$. We define the Rosseland mean opacity as $\kappa_R \equiv 1/\rho_0\lambda_R$, and set $\kappa_R = \kappa_0T^{-n}$. As presented in Refs. (1), it is then a straightforward exercise to find a similarity solution to Eq. (2), thus turning it from a P.D.E. into an O.D.E.and solving near the steep nonlinear heat front, we find:

$$T(x,t)=T_0\left(1-\frac{x}{x_M(t)}\right)^{\frac{1}{4+n-l}} \qquad (3)$$

where $x_M^2 \propto T^{4+n-l}\, t / \kappa_0$. For gold walls we find n=1 and l=3/2 to be reasonable fits (motivated shortly), thus Eq. (3) leads to:

$$T=T_0\left(1-\frac{x}{x_M(t)}\right)^{\frac{1}{3.5}};x_M\propto T_0^{1.75}\sqrt{\frac{t}{\kappa_0}} \qquad (4)$$

We see that the temperature profile is flat until very near the heat front where it nose-dives to zero, and that the front position, $x_{M(t)}$, moves into the wall with the expected $t^{1/2}$ diffusive behavior. This heat front position is referred to as the Marşhak depth., named after the late Robert E. Marshak whose paper in Phys. Fluids **1**, 24 (1958) was a landmark contribution to this field.

Most reasonable choices for n and l lead to similar flat-topped, steep fronted T profiles. The particular choices for l and n are derived from fits to LASNEX data. We find l=3/2 a reasonable result since $\varepsilon \propto ZT$ (where Z is the ion charge state) and $Z \propto T^{1/2}$ by simple arguments of temperatures being of order the ionization potential which scales as Z^2. For the average atom XSN opacity model in LASNEX, we find we can fit XSN's κ_R as varying as 1 / T , thus, n=1.

We now investigate the wall loss scaling. The wall loss E_W is given by the product of the specific energy ε with the heated mass, which is ρx_M times the wall area A_W. Thus,

$$E_W \propto \varepsilon \cdot (\rho x_M) \cdot A_W \propto T^{1.5} \cdot T^{1.75} \sqrt{t/\kappa_0} \propto T^{3.25} \sqrt{t/\kappa_0} \qquad (5)$$

from which we can derive the scaling of absorbed energy flux,

$$\dot{E}_W \propto T^{3.25} / \sqrt{t\kappa_0} \qquad (6)$$

Note too that we could have derived this flux from a different but equivalent point of view. Recall our discussion following Eq. (2):

$$Flux \propto \frac{T^4}{x/\lambda_R} \propto \frac{T^4}{x_M \rho \kappa} \propto \frac{T^4}{T^{1.75}\sqrt{\frac{t}{\kappa_0}\frac{\kappa_0}{T}}} \propto \frac{T^{3.25}}{\sqrt{t\kappa_0}} \qquad (7)$$

which gives the same result as Eq. (6). [Note that we have been a bit "sloppy" in ignoring the difference between T(x,t) and the boundary value $T(x=0,t)=T_0$. This is because of the nearly flat

T profile, which makes T(x,t) nearly identical to T_0=T(x=0,t) for almost all of $x < x_M$, namely for all of x within the heat front.]

These results are rather well known in the field and I refer to them as the old paradigm, in which the boundary value of T is constant in time. Note that with that constraint, the absorbed flux required to maintain the T decreases in time. Conversely, if a constant flux (driven, say, by a flat top laser drive)were impinging on a wall, and there were no other sinks for this flux, the wall would absorb this constant flux. Since the losses decrease in time at constant T, this constant absorbed flux would result in a temperature in the wall that would rise. This is far more realistic a situation for flat top laser drive, and the implications of this simple fact will be addressed shortly.

As a useful digression, let us now define a useful quantity, the wall reflectivity or albedo α.

$$\alpha \equiv \frac{\dot{E}_{out}}{\dot{E}_{in}} = \frac{\dot{E}_{out}}{\dot{E}_{out} + \dot{E}_W} = \frac{\alpha T^4}{\alpha T^4 + \dot{E}_W} = \frac{1}{1 + \frac{const.}{\alpha T^{0.75}\sqrt{t\kappa_0}}} \qquad (8)$$

Here we have assumed that a flux T^4 is incident on a wall (a convenient system of units, to be discussed later, has σ = 1) so that by definition, αT^4 is the flux that is reflected. From Eq. (8) we see that the albedo approaches 1 for long times, large T, or large opacity. In any of those three cases, the number of mean free paths in the diffusive heat wave increases, presenting an increasingly difficult barrier for the thermal wave to diffuse inward, thus decreasing the net absorbed flux and correspondingly increasing the reflectivity to approach unity. Thus for the NIF targets where the drive is on for a relatively long time, the wall loss will decrease allowing better coupling to the capsule. There are other important implications of Eq. (8). If we measure the albedo at a given T and t, we are essentially measuring the opacity coefficient, κ_0. Any future wall loss in the NIF at a longer pulse but at the same T will follow from Eq. (8), thus

making the measurements performed on Nova (at the same T as the NIF) extremely relevant and useful. These experiments and concommitant LASNEX simulations will be discussed in Sections III and IV.

It may be instructive to consider albedo from a different but equivalent perspective. We see from Eq. (4) that the temperature drops from its boundary value to zero at the heat front. A detector looking into the wall will see 1 optical depth into that temperature profile and see a T less than T_0. Effectively the wall will be "radiating" at a T lower than T_0 and that ratio to the 4th power is the albedo.

$$T = T_0\left(1-\frac{x}{x_M}\right)^{\frac{1}{3.5}} = T_0\left(1-\frac{x/\lambda_R}{x_M/\lambda_R}\right)^{\frac{1}{3.5}} = T_0\left(1-\frac{\tau}{\tau_M}\right)^{\frac{1}{3.5}} \tag{9}$$

where τ represents the optical depth, and τ_M representsthe number of optical mean free paths within the Marshak depth. Thus

$$\alpha = \frac{T(\tau=1)^4}{T_0^4} = \left(1-\frac{1}{\tau_M}\right)^{1.14} \approx 1-\frac{1.14}{const.T^{0.75}\sqrt{t\kappa_0}} \tag{10}$$

which goes to the same limits as the formulation of Eq. (8) when α is near unity. In Eq. (10), $\tau_M = x_M/\lambda_R = x_M\rho\kappa_R$ is derived in the same way it is in the denominator of Eq. (7). More formally, the albedo can be derived via this approach by solving the transfer equation:

$$\alpha = \frac{\int_0^{\tau_M} T^4 e^{-\tau} d\tau}{T_0^4} \approx 1-\frac{\left(1-e^{-\tau_M}\right)}{\tau_M} \tag{11}$$

which for both large and small values of τ_M. goes to the proper limits of $(1-(1/\tau_M))$ and $(\tau_M/2)$ respectively.

The concept of albedo is useful in that we can parameterize the wall loss in terms of it, and with that, systematize hohlraum energy balance. Since α is reflectivity, $(1-\alpha)T^4$ is the flux not reflected, namely the wall loss (per unit area). Thinking globally then, a laser power P_L absorbed within a hohlraum is converted to soft x-rays with an efficiency η_{CE}. This source flux goes into the walls at a rate $(1-\alpha)T^4 A_W$ and out the laser entrance holes at a rate $A_H T^4$, where $A_{W,H}$ are the wall and hole areas respectively. Of course if there is a capsule in the hohlraum that would be an additional sink of energy. In summary, in an empty hohlraum, this simple source=sink model yields:

$$\eta_{CE} P_L = \left[(1-\alpha)A_W + A_H\right]T^4 \tag{12}$$

Later in this paper we will use this formulation to systematize a wide variety of observations of T vs. P_L, thereby coming to some conclusions as to the values of η_{CE} and α.

It should be noted that we have introduced a significant simplification here. The x-rays emitted from the laser illuminated spot have, in general, a hotter spectrum than the reemission from the majority of the hohlraum wall which is unilluminated by direct laser light. A more sophisticated two temperature hohlraum model is conceivable, but we believe that the simple one temperature model presented here is sufficient for putting a large body of hohlraum drive results into a simple systematics. This conclusion is demonstrated later in this paper by the agreement of the simple model systematics with LASNEX simulations (which provide a far more detailed description of the hohlraums than any two temperature model). Part of the reason for the success of the simple model is that the harder spectrum from the laser produced x-rays are quickly absorbed by the walls and reemitted as softer x-rays.

Another simplification introduced here is the neglect of convergent geometry. We have assumed planar expansions. In a hohlraum it is possible that later in time the radiation driven blowoff will stagnate and create a new source of x-ray emission and possibly send a pressure

wave back toward the high density region near the Marshak wave front. For the "scale 1" hohlraum sizes and the nsec timescales of interest in the bulk of the data base discussed later in this paper, we do not believe stagnation plays a major role in the enegy balance and is therefore ignored.

With these fundamentals as a base, we can now build up a more realistic picture of the wall loss in a real system. The first extra element to add to our picture is time dependence of T_0 (t) = T(x=0,t), which up to this point has been held constant in time. As we have seen from Eq. (6) or (7), the absorbed flux required to maintain such a constant T decreases with time as $t^{-1/2}$. As mentioned above, in a hohlraum driven by a laser pulse with a "flat-top" temporal power profile, a flux of x-rays that is either constant or slightly increasing with time will be produced. As this incident flux is absorbed by the walls, it is more than sufficient to maintain a constant T, so in fact T will rise. A short cut at deriving the time dependence of that rise, is to set the flux of Eq. (6) or (7) equal to a constant in time. That requires T to scale as $t^{1/6.5}$. As we shall see, this weak but noticeable rise with time is in good agreement with experimental observations. What also follows from this behavior is that the Marshak depth, x_M, no longer scales as $t^{1/2}$ (see Eq. (4)), because of the time dependence of T. Inserting that $t^{1/6.5}$ dependence of T into Eq. (4) we find x_M scaling as $t^{0.77}$, much closer to the nearly linear dependence of burn-through times with sample thickness that is observed in albedo experiments to be discussed later. Another quantity of interest that does not chage too dramatically is the time dependence of 1-α. When α is near 1 (which is typical) Eqs. (8) or (10) or (11) predict a scaling of 1-α as $1/T^{.75}t^{1/2}$, so the previously predicted $t^{-1/2}$ behavior for that quantity (when T was constant in time) is now, with T scaling as $t^{1/6.5}$, slightly modified to be $t^{-0.61}$.

The next level of complication necessary for a more accurate description of our experiments, is to account for the change in density of the wall material. As the Marshak wave soaks into the solid wall, the heated portion blows back outward into near vacuum, thus

producing a density profile that must self consistently be accounted for in the solution to Eq. (2). Up to this point in our presentation we have artificially set the density ρ to be constant in time and space. A way to still obtain similarity solutions is to set ρ equal to $\rho_0 x_M / C_s t$ (where C_s is the sound speed of the heated material at temperature T and scales as $\varepsilon^{0.5)}$. This formula for ρ represents the idea that an amount of solid material (originally at solid density ρ_0) heated to a depth x_M, is now spread out over a distance $C_s t$ after a time t, and is thus at the lower density ρ. Along with this necessary complication we must generalize the power law dependencies of ε and κ_R to include ρ in addition to T, namely $\varepsilon = \varepsilon_0 T^{l} \rho^{-Q}$ and $\kappa_R = \kappa_{R0} T^{-n} \rho^{R}$. For Au we find Q = 0.2 and R = 1/3. The sign of the dependence of ε on ρ can be understood from the LTE notion that higher density drives recombinaton of the free electrons back down into the ions, lowering the ionic charge Z and lowering the specific heat due to the free electrons. Redoing the similarity solutions with these more complicated scalings, (again, details can be found in Refs (1)) yields:

For T constant in time:

$$E_W \propto T^{3.0}\, t^{0.63}\, \kappa_0^{-0.37}$$

$$\rho_0 x_M \propto T^{1.7}\, t^{0.53}\, \kappa_0^{-0.47} \qquad (13)$$

$$(1-\alpha) \propto 1/T \quad t^{0.37}\, \kappa_0^{\,0.37}$$

For Absorbed Flux that is constant in time: $(T \propto t^{0.12})$

$$E_W \propto T^{3.0}\, t \quad \kappa_0^{-0.37}$$

$$\rho_0 x_M \propto T^{1.7}\, t^{0.74}\, \kappa_0^{-0.47} \qquad (14)$$

$$(1-\alpha) \propto 1/T \quad t^{0.48}\, \kappa_0^{\,0.37}$$

We have tested these scalings by performing LASNEX simulations of test cases of Marshak waves in gold. Before presenting those results, let us first introduce convenient "hohlraum units' in which T is measured in hectovolts (hundreds of eV), area in mm^2, time in ns, mass in gm and energy (a bit clumsily) in hectojoules. With these units, as alluded to in the discussion following Eq. (8), $\sigma = 1$, and normalized irradiance is 10^{13} W / cm^2 (=hJ/mm^2 ns = 10^2 J /10^{-2} cm^2 10^{-9} s) and similarly, normalized power is 10^{11} W (=hJ/ns = 10^2 J /10^{-9} s). In these units, we find the LASNEX test problems, using XSN opacities whose κ_R in (cm^2/gm), can be fit as 3500 $\rho(gm/cm^3)^{0.33}$/ T(heV) yield:

For T const. in time: $E_W = 0.6\ T^{3.2}\ t^{0.67}\ \kappa_0^{-0.37}$ (hJ/mm^2)

$$\rho_0 x_M = 1.8 \times 10^{-3} T^{1.7} t^{0.57} \kappa_0^{-0.47} (gm/cm^2) \quad (15)$$

$$(1-\alpha) = 0.52 / T^{0.37}\ \kappa_0^{0.37}$$

where κ_0 represents a multiplier on the opacity. The XSN fit was based on XSN results taken for 100eV < T < 300 eV and .01 gm/cc < ρ < 10. gm /cc. The LASNEX simulations were run for a similar range in T, for 1 nsec pulses impinging onto initially solid gold, and for opacity multipliers between 1 and 3.

Using Eq. (15) we find, for example, at 1 ns (t=1), a 260 eV source (T= 2.6), at nominal opacity, ($\kappa_0 = 1$) would yield a (1-α) of 0.2 or an albedo of 0.8. Comparing Eqs. (15) with (13) we see a fairly close agreement of power dependencies between our simplified approach to the problem and the detailed, multigroup radiation transport answer from LASNEX. For test problems with constant absorbed flux, we find:

For $T \propto t^{0.1}$: $E_W = 0.44\ T^{3.2}\ t\ \kappa_0^{-0.37}$ (hJ/mm^2)

$$\rho_0 x_M = 1.6 \times 10^{-3} T^{1.7} t^{0.8} \kappa_0^{-0.47} (gm/cm^2) \quad (16)$$

$$(1-\alpha) = 0.57 / T \quad t^{0.42} \kappa_0^{0.37}$$

where we see the LASNEX opinion of how time dependence of T leads to changes between Eqs. (16) and (15) similar to those changes we predicted between Eqs. (14) and (13). Note too the coefficients for wall loss are lessened in Eqs. (16) vs. (15) because with (16), if we have arrived at T at time t, it implies the system spent its previous history at a temperature less than T, thus there should be less loss.

More sophisticated opacity treatments are available to us, for example the STA (Super Transition Arrays) code which has a far more detailed treatment of bound bound opacity than the average atom XSN code, but can only be run in LASNEX in LTE via a look up opacity table. We are grateful to Bill Goldstein of LLNL for supplying us with the gold STA table. We find we can fit STA's κ_R in (cm^2/gm) to 6000 $\rho(gm/cm^3)^{0.3} / T^{1.5}$. This gives opacities quite close to XSN at T=3 heV, but at 100 eV (T=1) we see a difference of 2 between code predictions. The formalism we have presented can be redone for this STA opacity model. Basically the stronger power law for T in κ_R leads to a slightly higher power law dependence of E_W and $\rho_0 x_M$ on T, namely an additional 0.2. Indeed, the LASNEX simulations with STA confirm that. For example for STA we find:

For T const. in time: $E_{W(STA)} = 0.5 T^{3.4} t^{0.67} \kappa_0^{-0.37}$ (hJ/mm^2) (17)

The fits of STA and LASNEX were done under the same range of variations as described for the XSN results. In Eq. (17), note the change from $T^{3.2}$ to $T^{3.4}$ as predicted. Note too the coefficient for wall loss is smaller for STA than for XSN by 20%, and can be derived quite easily by considering the respective opacity coefficients, and calculating $(6000/3500)^{-0.37}$ as predicted by the κ_0 scaling. Of course the actual value of E_W for either case at T=3 is quite close, as we would expect given the two opacity models' agreement at T=3. For completeness, we quote:

For $T \propto t^{0.1}$: $E_{W(STA)} = 0.35\, T^{3.4}\, t\, \kappa_0^{-0.37}$ (hJ/mm^2) (18)

Before embarking on a discussion of the experimental data base it may be instructive to go through a numerical exercise in using some of these equations to find the T of a given hohlraum. Consider a cylindrical hohlraum of length 2.55 mm and diameter 1.6 mm, with laser entrance holes on either endcap of 0.8 mm diameter, and a diagnostic hole of 0.5 mm diameter. This means A_W is 15.8 mm^2 and A_H is 1.2 mm^2. A flat top laser power of 30 TW, on for 1 ns (therefore 30 KJ) irradiates the hohlraum. LASNEX calculations, to be described below, find a conversion efficiency into soft x-rays of about 70% by the end of the pulse. It also finds an albedo then of about 0.8. Thus the lhs of Eq. (12) would yield (0.7 x 300 =) 210 in normalized power units of 10^{11} W (= hJ/ns recall the discussion of units following Eq. (14)). The rhs would be (0.2 x 15.6 + 1.2) x T(heV)^4 , or 210= 4.3 T^4, or T=2.65, (namely 265 eV) quite close to what turns out to be LASNEX predictions (and the data!). A different approach would be an energy balance rather than power balance consideration:

$$\eta E_L = E_W + E_H \qquad (19)$$

where E_W is given by Eq. (16) and E_H can be found by:

$$E_H = A_H \int_0^t \left(T_0 \left[\frac{t}{t_0} \right]^{0.1} \right)^4 dt = A_H \frac{1}{1.4} T_0^4 \left(\frac{t^{1.4}}{t_0^{0.4}} \right) \qquad (20)$$

Thus, for our problem we have (at $t=t_0=1$) :

$$0.7\,(300)\,(\text{hJ}) = (0.44 \times T^{3.2}\,(\text{hJ/mm}^2) \times 15.6\,(\text{mm}^2)) +$$

$$(0.71 \times T^4\,(\text{hJ/mm}^2) \times 1.2\,(\text{mm}^2))$$

or: $210 = 6.9\, T^{3.2} + 0.9\, T^4$

whose solution, T=2.7, is quite close to the previous result and to the data.

III Experiments and LASNEX Simulations on Drive :

The hohlraum temperature is measured in two independent ways. An aluminum wedge witness plate is placed on the hohlraum wall. The radiation ablates away at the Al that faces the hohlraum interior, launching a shock wave that propagates through the aluminum, eventually to break-out to the wedge shaped backside that faces the outside world. An optical pyrometer, streaked in time, records the optical emission that ensues upon shock breakout. The wedge shape allows us to measure the shock speed continuously throughout time. The shock speed is indicative of the drive, which is derived via comparison with LASNEX simulations. The EOS of aluminum is sufficiently well known to make this a very powerful and accurate technique. These experiments have been carried out by Chris Darrow and Don Phillion of LLNL.

A second method to measure drive involves the Dante sub-keV broadband spectrometer. Approximately 10 broadband filtered channels cover the entire sub keV spectrum in which the bulk of the emission occurs. The Dante looks at a laser-unilluminated portion of the wall, and thus sees a radiation heated wall reemitting as αT^4. Thus, Dante must be corrected for albedo if it is to be directly compared with a measurement of drive such as would drive a capsule or the Al wedge witness plate. The Dante is time resolved with about 100 psec resolution. These experiments have been carried out by Harry Kornblum of LLNL.

We use the 2-D hydrodynamic simulation code LASNEX to model the drive in hohlraums. These simulations were carried out by Ron Thiessen of LLNL, and the details of the simulation technique as well as extensive comparisons with a large data base, will be

published elsewhere.[2] Nominal gold opacities, as calculated by the XSN average atom package in LASNEX are used. The problems are run either non LTE or LTE with very little difference in results.

The problems, once run to completion are post processed in a variety of ways to mimic the measurements. The TDG post processor can, for instance, look into a wall just as the Dante channels do, and the time evolution of the spectrum (which is roughly Planckian) and its frequency integral, the drive, characterized by a T_R derived from the fourth root of the energy flux, can be directly compared with the measurement. Moreover, the drive derived from the calculation can be applied, in a subsidiary calculation, to a wedge of aluminum, and the predicted trajectory of the radiation ablation driven shock can be compared with the measurement as well.

In Fig 1 we compare the two measurements along with the respective LASNEX predictions for a 1 nsec flat top, 30 TW, scale 1 Au hohlraum. We see excellent agreement of LASNEX with both independent measurements. (Equally excellent agreement is seen in for a lower power irradiance of 10 TW.) It is important to note the slight rise with time of T_R despite the laser power being flat in time. This behavior was predicted in Section II when the constant absorbed flux boundary condition is used. Quantitatively, we expected a $T \propto t^{0.1}$ behavior, and we observe in the data and in the simulation something closer to a $T \propto t^{0.15}$ behavior instead. This is probably due to the fact the flux is not constant, despite the laser power being flat topped, due to the conversion efficiency having a slight dependence on time. Thus the x-ray source flux increases slightly in time, leading to a slightly larger power depence of T on t. The implication of this on the burnthru time, to be discussed in the next section, can be anticipated by inspecting the second line of Eq. (16). The expected $X_M \propto t^{0.8}$ will increase to about an $X_M \propto t^{0.9}$ since the power law of T with t is slightly higher than assumed. As we shall see presently, this is precisely what is observed!

IV Experiments and LASNEX Simulations on Wall Loss :

To study wall loss more fundamentally we have performed a series of measurements, looking at the burn-through times of thin patches of gold (1 to 3 μm) stretched across a hole in the hohlraum wall (which is typically 25 μm thick). The shorter the measured burn-through time (at a given thickness and drive) the lower is the inferred Rosseland averaged gold opacity. The observations have been made with the 10 channels of Dante at a given drive and thickness, and also with a spatially resoved, single channel detector, which allows, for the same shot (and drive) a measure of the burn-through times through several different thickness patches, all aligned along the side of the hohlraum. These experiments were designed by Ron Thiessen of LLNL, and carried out by John Porter of LLNL, and will be published shortly.[3]

Burn-through time is defined as the time when the signal rises to half its peak value. In Fig. 2 we plot the results of burn-through time vs, thickness for two energy channels. LASNEX simulations used the measured drive and via TDG post processing simulated the burn-through signal for the appropriate channels, and defined burn-through time the same way the experiment did. The LASNEX curves are also plotted in Figure (2). Note the excellent agreement between LASNEX and the data, and how a choice of opacity multiplier of 2.5 is clearly discriminated against by the data. The errors due to drive uncertainty etc lead to a tight 30% uncertainty in opacity. Note too the nearly linear relationship between burn-through time and thickness, a consequence of a T_R rising in time (recall our discussion at the end of the previous section). These experiments were originally motivated under the old paradigm of Eq.(4) in which we expected the burn-through times to scale as thickness squared, and to be sensitive linearly with opacity. As the new paradigm (Eq. (16)), and the data, and LASNEX, indicate, the experimental burnthrough isn't quite that optimistically sensitive to thickness

and opacity- it scales linearly with thickness, and as the square root of opacity. Nonetheless, that is good enough to tie down the opacity to 30%.

As an additional check on the XSN opacity we reran the calculations using the LTE STA opacity package, available to be run in LASNEX via a look-up tabular opacity. The STA code is far more sophisticated than the average atom XSN code, and cannot be run non-LTE in line with LASNEX. Note that STA results, also in Fig. 2 give nearly identical results as the XSN, another comfirmation of XSN's veracity. When we compare the detailed opacity of the two codes and see that indeed at 260 eV they give the same Rosseland mean opacity. As mentioned in Section II, the two codes give different predictions at 100 eV, and burnthrough experiments such as these, redone at 100 eV would be most illuminating. For the record we note that the good agreement between LASNEX and data persist for all the other Dante channels as well. Also for the record we note that independent experiments, in which the shock breakout of a radiation ablation driven shock is monitored through thick samples of gold are also consistent with nominal opacities.

V Summary

We have seen that the constant absorbed flux boundary condition leads to several qualitative differences in predicted scaling when compared with the old paradigm of constant temperature. In particular the rise of T with time is predicted, and is observed in both simulation and measurement of hohlraums driven by flat top pulses. Moreover, with this slight rise of T with time, due to the non linear dependence of the Marshak depth with T, the paradigmatic, diffusive $x_M = t^{1/2}$ behavior now changes to one nearly linear with time, an effect indeed observed by experiment and simulation.

We gratefully acknowledge useful conversations with our LLNL colleagues R. Thiessen, C. Darrow, H. Kornblum, J. Porter, B. Goldstein, and L. Suter, as well as with our AWE colleagues B. Thomas and P. Thompson. This work was performed under the auspices of the U.S. Department of Energy, by the Lawrence Livermore National Laboratory under contract W-7405-ENG-48.

Figure captions

Figure 1. a) T vs. time as measured by Dante and as simulated by LASNEX. b) The data is confirmed by the Aluminum wedge witness plate shock breakout vs. time that is also matched by the LASNEX simulations.

Figure 2. Burn through time of thin Au vs. Au thickness for two Dante-like broad band channels at 250 and 500 eV.

REFERENCES

[1] M.D. Rosen "Scaling Laws for Hohlraum Drive" (Title (U), Report SRD) UCRL-50055-79 pp 2-37 to 2-46 (1979); M.D. Rosen "A Model for Albedoes Based on Simple Marshak Wave Scaling Laws" (Title (U), Report SRD)(see especially Appendix A) COPD 81-133 (1981)and UCRL 50055-81/82 pp 2-3 to 2-6 (1983); Especially recommended for clarity and completeness is S.J. Davidson and B.R. Thomas (AWRE) "Heating of Laser Targets: Part I" (Title (U), Report UK SAP) SPE Note 8/84 [ACO (UK)7573] (known colloquially as "Rosen Revisited") 1984

[2] R. Thiessen, C. Darrow, H. Kornblum, and D. Phillion, to be published in the 1992 Classified ICF/Laser Program Annual Report.

[3] J. Porter, R. Thiessen, and M. Rosen, to be published in the 1992 Classified ICF/Laser Program Annual Report.

Drive from Au hohlraums is in accord with 2-D LASNEX simulations

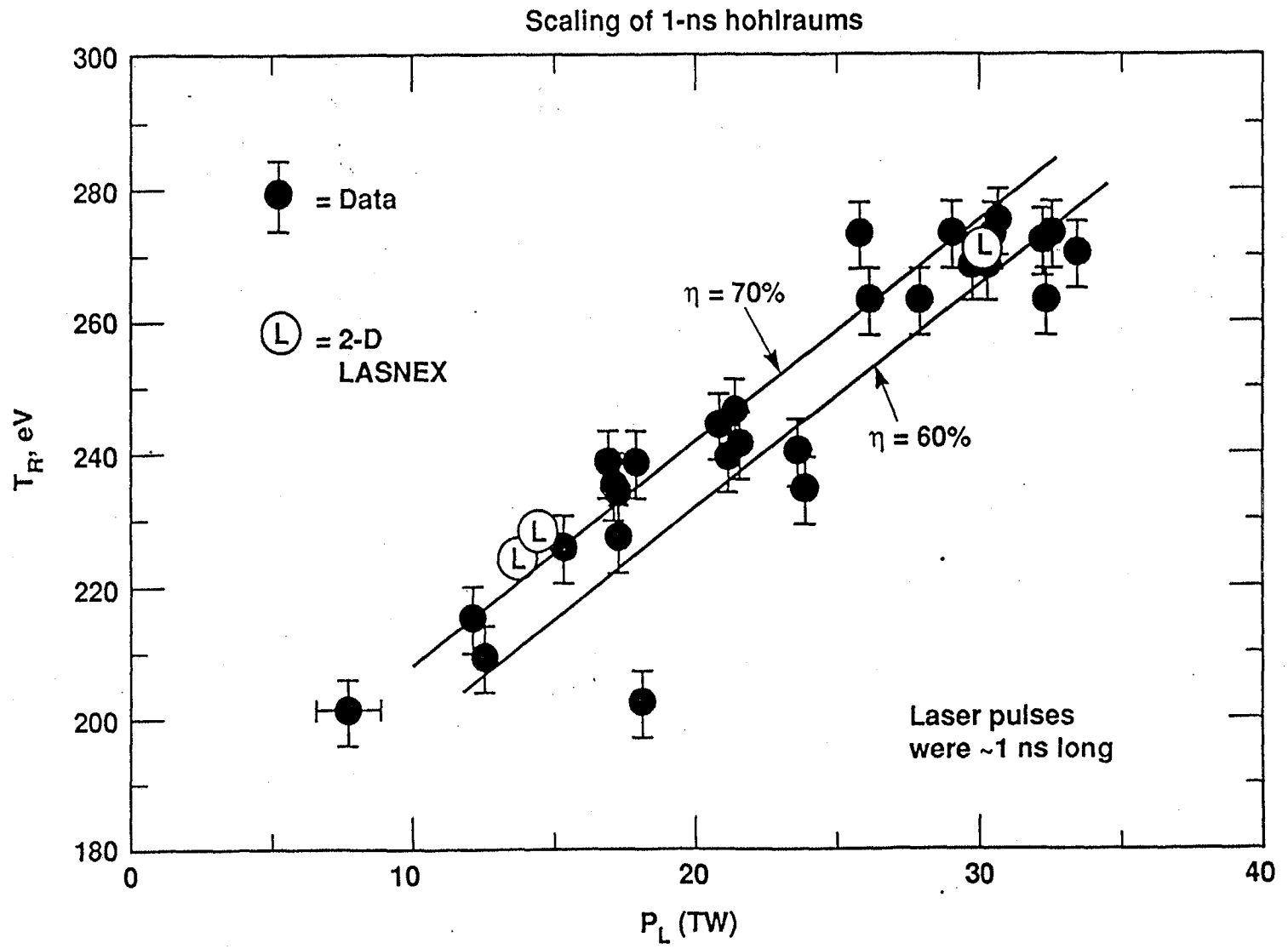

50-00-0592-1542F

The radiation-wave burnthrough measurements in thin Au foils agree well with the default XSN calculations

Streaked XUV imager data at hν = 550 eV

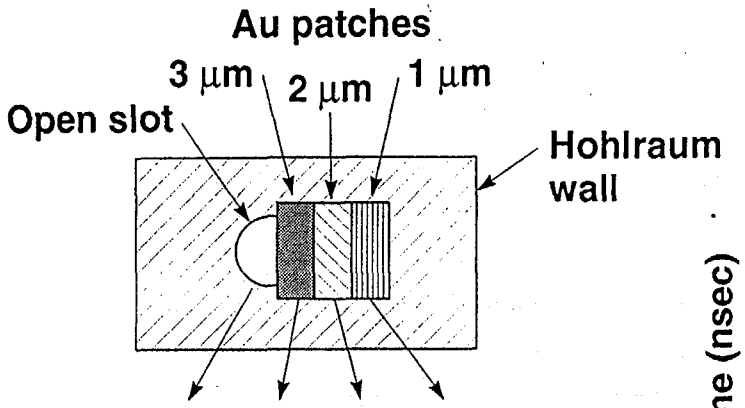

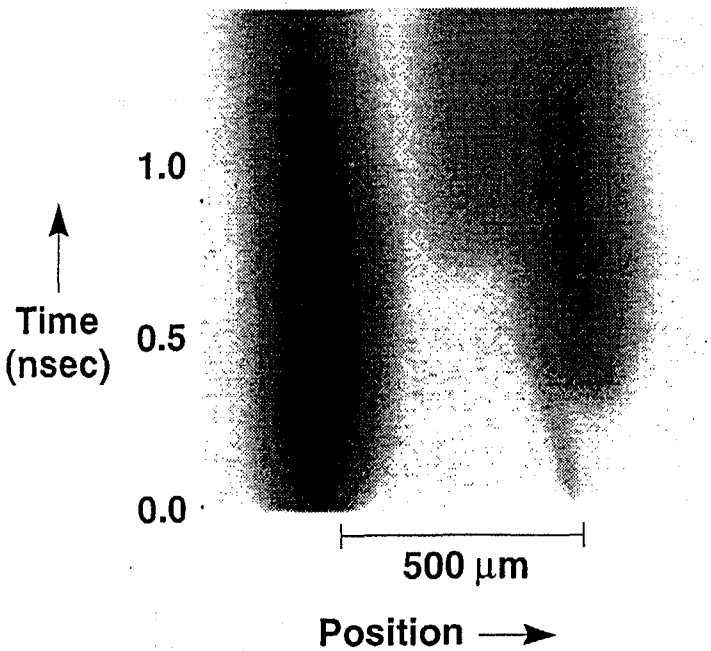

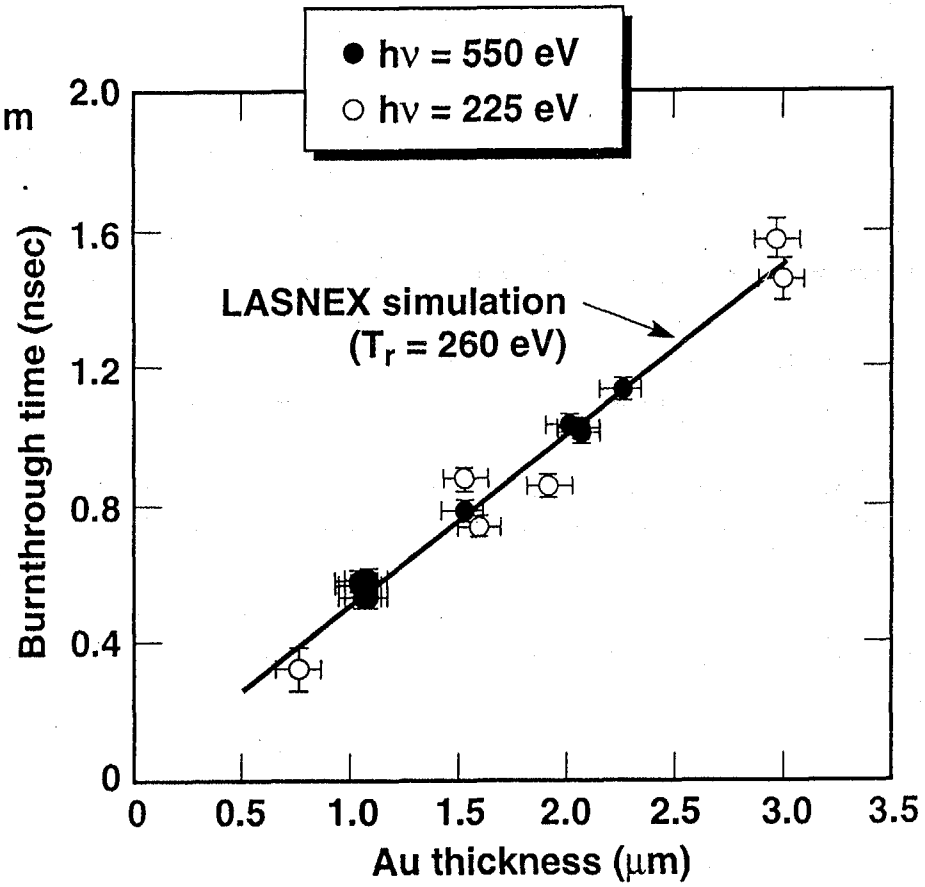

R. Sigel, H. Nishimura, et. al
Phys. Rev. Lett (1990)
J. Porter, R. Thiessen (LLNL,1990)